ANALYSIS OF SEISMIC RESPONSE OF FULLY GROUTED REINFORCED CONCRETE MASONRY SHEAR WALLS

M. T. Shedid[1], W. W. El-Dakhakhni[2], and R. G. Drysdale[3]

[1] *Ph.D. Candidate, Dept. of Civil Engineering, McMaster University, Hamilton. Ontario, Canada*
[2] *Assistant Professor, Martini, Mascarin and George Chair in Masonry Design, Dept. of Civil Engineering, McMaster University, Hamilton. Ontario, Canada*
[3] *Professor Emeritus, Dept. of Civil Engineering, McMaster University, Hamilton. Ontario, Canada*
Email: shedidmmt@mcmaster.ca, eldak@mcmaster.ca, drysdale@mcmaster.ca

ABSTRACT :
This paper presents detailed analyses of an experimental study conducted to evaluate the possibility of achieving high levels of ductility and energy dissipation in reinforced concrete masonry shear walls failing in flexure. The test program consisted of testing six reinforced concrete masonry shear walls to failure under reversed cyclic lateral loading. The current study focuses on documenting the levels of ductility attained by the walls, evaluating the contribution of flexure and shear deformations to the overall wall lateral displacement, and estimating the amount of energy dissipated by hysteretic damping. The measured and predicted wall capacities are discussed with respect to the MSJC code (2005) and the CSA S304.1 (2004). Analysis of the measured displacements showed that the shear displacement contribution of the test walls (all with height-to-length ratio of 2.0) to the overall wall displacement was significant but was not the same for all the walls. It was also shown that reinforced masonry shear walls can exhibit high levels of energy dissipation.

KEYWORDS: Ductility, Energy dissipation, Shear Walls, Masonry

1. INTRODUCTION

In regions where strong ground motions are anticipated, it is generally not economical to design shear wall buildings to remain elastic during a severe earthquake. Therefore, during a moderate to high seismic event, inelastic deformations are expected which result in a significant reduction in the walls' seismic demand. For cantilever reinforced masonry shear walls, a ductile response can be achieved through the development of a flexural plastic hinge at the base of the wall which also results in a significant amount of energy dissipation (Drysdale and Hamid 2005).

Currently, most seismic design methodologies rely on using prescriptive requirements that allow reduction in seismic design forces calculated based on elastic behavior to account for the effect of ductility in the structure. In the Masonry Standards Joint Committee code (MSJC 2005) in the United States and in the Euro-code (EC8), similar values for this ductility modification factor, *DMF* are assigned to reinforced concrete and reinforced masonry shear wall buildings. In the National Building Code of Canada (NBCC 2005), reinforced masonry shear wall construction is considered to be relatively brittle compared to reinforced concrete shear wall construction. The Canadian code assigns *DMF* values of 2.0 and 3.5 for moderately ductile masonry shear wall buildings and for ductile reinforced concrete shear wall buildings, respectively. Therefore, the reinforced concrete building is designed for 57% of the lateral load on the masonry building. The conservative Canadian values assigned to masonry shear wall structures may be mostly attributed to the poor performance of *unreinforced* masonry during past earthquakes (Priestly 1986). On the other hand, some studies indicated that a ductile response, which should reduce that demand by increasing the value of the *DMF*, is attainable. Englekirk and Hart (1982) proposed a displacement ductility of 1.5 and 3.0 for the serviceability limit state and the ultimate strength limit state, respectively, for reinforced masonry shear walls. Moreover, results of some research programs indicate that reinforced masonry shear walls, when properly proportioned, and constructed, provide reasonable ductility and adequate safety against seismic forces (Abrams 1986). The investigation presented herein indicates that, a displacement ductility of 3.0 can easily be attained with only minor degradation in wall capacity for high reinforcing ratios and much higher ductilities are possible for more moderate amounts of reinforcement.

2. EXPERIMENTAL PROGRAM

The experimental program focused on investigating the flexural response of six fully-grouted 1.8 m × 3.6 m reinforced concrete masonry shear walls constructed using 190 mm normal weight concrete blocks. The walls were tested under displacement-controlled cyclic loading simulating earthquake effects. All walls were tested to 50% degradation in strength to obtain information about the post-peak behavior, ductility, and stiffness degradation trends.

A summary of the reinforcement ratios, number of bars, and levels of applied axial compressive stress for the test walls is given in Table 2.1, along with the predicted and measured wall capacities. The flexural and shear reinforcement ratios, ρ_v and ρ_h, respectively, are the areas of the reinforcing steel divided by the gross area of the horizontal and vertical masonry cross section, respectively. Predictions of the flexure capacity, Q_u, in Table 2.1 are calculated based on the guidelines of the MSJC code (2005) and the Canadian Standards Association "*Design of masonry structures"* CSA S304.1 (CSA 2004). Flexure capacity is defined as the top lateral force that will cause flexural failure at the wall base and is calculated based on beam theory.

Table 2.1: Summary of wall details and capacities

Wall	Vertical reinforcement		Horizontal reinforcement		Compressive Stress (MPa)	Predicted Q (kN)				Measured Q (kN)	
	No. and size	ρ_v (%)	No. and spacing	ρ_h (%)		CSA (2004)		MSJC (2005)		Q_y (- ve)	Q_u (- ve)
						Q_y	Q_u	Q_y	Q_u		
1	5 #15[2]	0.29	#10[1] @ 600 mm	0.08	0	84	119	84	120	95 (84)	143 (122)
2	9 #20[3]	0.78	#10 @ 400 mm	0.13	0	186	268	189	268	185 (182)	265 (246)
3	5 #25[4]	0.73	#10 @ 400 mm	0.13	0	188	262	191	262	174 (190)	242 (235)
4	9 #25	1.31	#10 @ 200 mm	1.13	0	291	399	295	396	296 (292)	360 (380)
5	9 #25	1.31	#10 @ 200 mm	0.26	0.75	330	424	336	420	311 (316)	377 (407)
6	9 #25	1.31	#10 @ 200 mm	0.26	1.50	410	480	424	471	450 (455)	541 (558)

[1] No. 10 = 100 mm^2 [2] No. 15 = 200 mm^2 [3] No. 20 = 300 mm^2 [4] No. 25 = 500 mm^2

2.1. Material Properties

The average compressive strength of the grouted 4-block high masonry prisms, f'_m, was 14.8 MPa (*c.o.v. = 4.4%)*. In accordance with CSA (2004), this value would be the basis for choosing design strength values, whereas for the MSJC code (2005), where 2-block high prisms (height to thickness ratio of 2) are considered to represent masonry compressive strength in the wall, the 4 block high prism results would be modified to be 14.8 × 1.15= 17.0 MPa. The average yield strength for the vertical reinforcement used in all walls was 502 MPa (*c.o.v* = 0.6%) except for the vertical reinforcement used in Wall 6, which was obtained separately and had an unexpected yield strength of 624 MPa.

2.2. Test Setup and Instrumentation

Figure 1 shows the test setup with the wall foundation prestressed onto a larger reinforced concrete slab which was, in turn, prestressed to the laboratory' s structural floor. At the top of the wall, the vertical reinforcement extended through and was welded to a U-shaped built-up steel loading beam. The lateral load was supplied

through a displacement controlled 1,400 kN hydraulic actuator with its centerline aligned with the top of the wall. Rollers were attached to the out-of-plane bracing in order to prevent out-of-plane displacement while providing no resistance to in-plane displacement.

During testing, loads, displacements and strains were recorded using a computerized data acquisition system. As shown in Fig. 1, 29 displacement potentiometers were used to monitor the vertical, horizontal and diagonal displacements of the masonry as well as the slip with respect to the wall foundation. Lateral displacements relative to the wall foundation were measured using potentiometers attached at eight different heights to a truss system which was supported on the wall foundation. Vertical displacements with respect to the wall foundation were measured using 7 potentiometers at each wall end installed vertically over the wall height, and diagonal displacements were measured by the two diagonal potentiometers extending from the corners of the walls. In addition to the external instrumentation, 10 strain gauges were attached to the outermost reinforcing bars within the most highly stressed region to investigate the extent of yielding over the wall height and inside the concrete foundation, as well as identifying the yield displacement.

The cyclic loading scheme adopted for all tests consisted of a series of displacement-controlled loading cycles to assess the strength and the stiffness degradation at each displacement level. The walls were cycled twice at each displacement level. To obtain information that included the post-peak behavior, displacements were increase incrementally until the specimen had achieved maximum lateral load resistance and then lost about 50% of its maximum capacity.

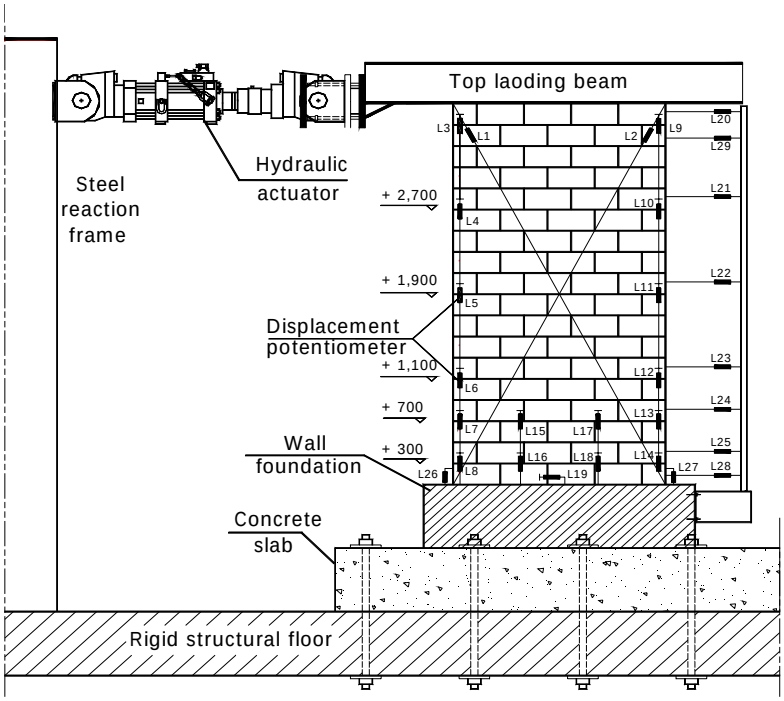

Figure 1 Test setup and external instrumentation

3. EXPERIMENTAL RESULTS

All walls behaved in an almost linearly elastic manner up to the onset of yield of the outermost bar. This resulted in thin hysteresis loops which are characterized by low energy dissipation, as shown in Fig. 2 for selected walls. At higher displacement levels, the area within the hysteresis loops increased indicating higher levels of energy dissipation and increased inelastic deformation due to damage. For loading beyond the initial yield displacement, the second cycle of loading resulted in less resistance corresponding to the same displacement. However, as can be seen, increasing the displacement to the next increment consistently resulted in regaining the previous resistance up to the displacement at which significant damage was clearly visible.

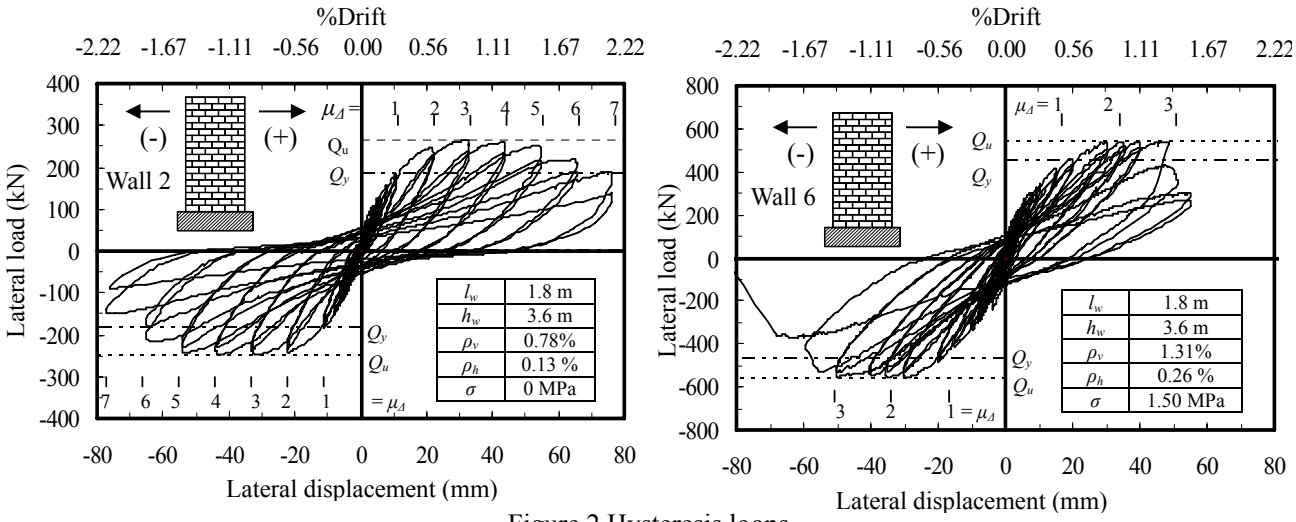

Figure 2 Hysteresis loops

3.1 Wall Capacities

The predicted and experimentally measured yield strength, Q_y, and ultimate flexural strength, Q_u, of all walls are listed in Table 2.1. Predictions of strength were calculated including compression reinforcement, even though design codes recommend ignoring compression reinforcement unless it is adequately tied. Using beam analysis with strain proportional to distance from the neutral axis, these predictions were carried out twice, following both CSA S304.1 (2004) and the MSJC code (2005). There are three principal differences in these analyses. In CSA S304.1, the equivalent rectangular stress block uses a stress of $0.85\,f'_m$ whereas $0.80\,f'_m$ is used in the MSJC code. The depth of rectangular stress block is equal to 80% of the distance to the neutral axis in both cases. In CSA S304.1, the limiting extreme fiber compressive strain is 0.003 compared to 0.0025 in the MSJC code. Finally, in CSA S304.1, the masonry compressive strength is based on the compression test of a 4-block high prism, whereas, in the MSJC code, the compressive strength of masonry is calculated based in the compressive strength of a 2-block high prism.

The experimental results in Table 2.1 can be compared to the predicted values using both the Canadian (CSA, 2004) and American (MSJC, 2005) design codes without material strength or member reduction factors applied. Despite the higher masonry compressive strength (17.0 MPa vs. 14.8 MPa) and higher modulus of elasticity (900×17 vs. 850×14.8) for the MSJC code, the yield strength results are very similar and closely predict the measured values. Regarding ultimate strength, again, despite significant differences in the masonry compressive strength, height of equivalent rectangular stress block, and limiting compression strain, both the Canadian and the American strength predictions for reinforced masonry shear walls are in good agreement with the experimental results. In general, the test results indicate that the use of beam theory for flexural strength predictions is within acceptable accuracy for walls with capacity controlled by yielding of the reinforcement. The good predictions agree with previous research investigating flexural capacity of shear walls (Priestley 1986). The only exception to this was the strength predictions for Wall 6, which was subjected to axial compressive stress of 1.5 MPa ($0.10\,f'_m$) and had very high strength reinforcement. The yield and ultimate strengths were underestimated by 10% and 13%, respectively. This result may indicate that using beam theory to predict the capacity of members subjected to high axial compressive stress tends to underestimate the strengths which agrees with test observations reported by Priestley and Park (1987) for reinforced concrete columns and walls.

The measured flexural yield and ultimate capacities for Walls 1, 2, 3 and 4 (with steel ratios of 0.29%, 0.78%, 0.73% and 1.31%, respectively) are presented in Fig. 3 (a). The figure illustrates that, as expected, the flexural strength is very sensitive to the amount of vertical reinforcement. Comparing Walls 2 and 3, having almost the same percentage of vertical reinforcement but with a different spacing (No. 20 every 200 mm, ρ_v= 0.78%, and No. 25 every 400 mm, ρ_v= 0.73%, respectively), indicates that the flexural strength is mainly affected by the

amount of reinforcement and is not very sensitive to the distribution of bars along the wall length. This is consistent with previous research on reinforced masonry shear walls reported by Priestley (1986). Figure 3 (b) presents the flexural yield and ultimate capacities for Walls 4, 5, and 6, which were subjected to different axial compressive stresses but had the same steel ratio. Due to the higher yield strength of the reinforcement in Wall 6, the lateral resistance of the wall was multiplied by a factor of 0.89 to make the comparison between the walls more meaningful. Full details of the numerical procedure can be found elsewhere (Shedid 2006). The figure shows that the flexure strength is less sensitive to the increased axial compressive stress compared to increase in reinforcement ratio.

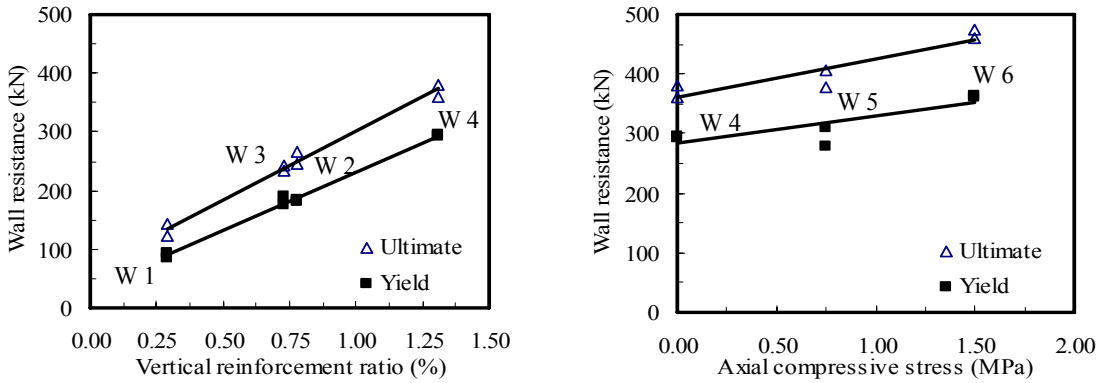

(a) Effect of amount of reinforcement (b) Effect of axial load

Figure 3 Wall resistances at the onset of yield and at ultimate capacity

3.2 Wall Displacements

The total in-plane lateral displacements for the walls results from three main components, namely: sliding (slip between the wall and the wall foundation), flexural, and shear displacements. For the test walls, displacements due to sliding were removed from the total displacement by subtracting the base slip from the lateral displacements. To quantify the contribution of the flexure and the shear displacements in the total lateral wall displacement, decoupling of the displacement was conducted.

The theoretical flexural displacements at yield, Δ_y, and at maximum load, Δ_u, for a cantilever wall with height h_w can be estimated assuming an elasto-plastic moment-curvature diagram over the wall height based on an equivalent plastic hinge length, l_p, and using the curvatures at first yield, φ_y, and at maximum load, φ_u, as follows:

$$\Delta_y = \varphi_y \frac{h_w^2}{3}, \qquad \Delta_u = \Delta_y + (\varphi_u - \varphi_y)\, l_p\, (h_w - 0.5\, l_p) \tag{3.1}$$

The predicted displacements, presented in Table 3.1, were calculated using the theoretical strain profile (curvature) at the onset of yielding and at maximum load, by setting the ultimate masonry compressive strain, ε_u, to 0.0025 and assuming an equivalent plastic hinge length, l_p, equal to the wall length, l_w, and to half the wall length, following the guidelines of the MSJC code, and the CSA S304.1, respectively. Specific properties of the stress block following the MSJC code and the CSA S304.1 were used independently for displacement predictions. Different values of f'_m, were used corresponding to each code as indicated earlier. The predictions of the flexural displacements at the onset of yielding and at maximum load are presented in Table 3.1. The displacements Δ_{fAy} and Δ_{fCy}, are the predicted flexural displacements for the walls calculated at the onset of yield of the outermost reinforcing bar, using Eqn 3.1, following the MSJC code and the CSA S304.1 guidelines, respectively. Using Eqn 3.1, the displacements Δ_{fAu} and Δ_{fCu}, in Table 3.1, are the predicted flexural displacements for the walls corresponding to ultimate masonry compressive strain, again following the MSJC code and the CSA S304.1 requirements, respectively. The total measured displacements for all walls, at the onset of yield of the outermost reinforcing bar, Δ_y, and at maximum load, Δ_u, are also listed in Table 3.1. To evaluate the flexural and the shear displacements separately, the total measured displacements had to be decoupled. The flexural displacements, Δ_{fE}, were computed from the experimentally obtained curvature profile

along the wall height. Average curvatures over the wall height were determined based on strain profiles at different levels along the wall height (using the 7 potentiometers at each wall end). The average curvature profiles over the wall height used in the calculation of the flexure displacements are presented in Fig. 4 at different lateral displacement stages for loading in both directions. The product of the average curvatures, φ_i, and the corresponding segment length, h_s, gives the segment rotations, θ_i, at the center of each segment. The summation of these rotations, θ_i, multiplied by the distances from the center of the segment to the top of the wall, h_i, for all segments, gives the flexural lateral displacements, Δ_{fE}, at the top of each wall as shown in Fig. 5.

The average flexural displacements for the test walls, Δ_{fE}, given in Table 3.1, are about 68% and 80% of the total displacements at the onset of yielding of flexure reinforcement and at maximum load, respectively. This indicates that the average shear displacement for reinforced masonry shear walls having a height-to-length ratio of 2.0 is around 32% to 20% of the total lateral displacement at the onset of yielding and at maximum load, respectively. The lower contribution of shear displacements at maximum load can be explained based on the response of walls dominated by flexural behavior. At maximum load, high inelastic curvature in the plastic hinge zone, resulting from yielding of the flexural reinforcement, contributes the most to the total lateral displacement.

Table 3.1: Summary of predicted and measured wall displacements

Lateral displacements (mm)	Wall 1	Wall 2	Wall 3	Wall 4	Wall 5	Wall 6	% Average displacement
Measured (Δ_y)	7.0	11.1	11.3	14.8	16.2	16.9	NA
Δ_{fAy} (Δ_{fAy}/Δ_y) %	7.9 112%	8.6 77%	8.5 75%	9.1 61%	9.5 59%	12.4 73%	76%
Δ_{fCy} (Δ_{fCy}/Δ_y) %	7.6 109%	8.4 76%	8.4 74%	8.9 60%	9.3 57%	12.3 73%	75%
Δ_{fEy} (Δ_{fEy}/Δ_y) %	5.6 80%	7.6 68%	7.4 65%	9.6 65%	9.1 56%	11.9 70%	68%
Measured (Δ_u) (-ve direction)	31.6 (-32.4)	32.9 (-33.2)	24.2 (-29.2)	29.8 (-29.1)	25.3 (-33.2)	29.9 (-34.2)	NA
Δ_{fAu} ($\Delta_{fAu}/\Delta_{u,min}$) %	64.8 205%	30.3 92%	34.1 140%	23.2 80%	20.6 81%	17.4 58%	109%
Δ_{fCu} ($\Delta_{fCu}/\Delta_{u,min}$) %	37.1 117%	20.0 61%	21.9 90%	16.5 55%	15.3 60%	14.8 49%	72%
Δ_{fEu} ($\Delta_{fEu}/\Delta_{u,min}$) %	27.2 86%	24.2 74%	20.9 86%	24.3 82%	---* 	21.5 72%	80%

* No values reported as a result of the early loss of vertical potentiometers

3.3 Energy dissipation

Energy dissipation through hysteretic damping, E_d, is an important aspect in seismic design since it reduces the amplitude of the seismic response and, thereby, reduces the ductility and strength demands on the structure. The energy dissipation, E_d, is represented by the area enclosed by the hysteresis loops at each displacement level (horizontally hatched), as shown in Fig. 6. The vertically hatched region in the same figure represents the elastic strain energy, E_s, stored in an equivalent linear elastic system. Given that the displacement histories were not identical for all walls (each wall was cycled at multiples of its initial yield displacement), comparing the energy dissipated with respect to a single hysteresis loop at a particular drift level cannot be used as a basis for comparison between the test walls. Previous research (Sinha et al. (1964)) showed that the envelope of the load-displacement hysteresis loops is relatively insensitive to the imposed displacement increments and to the number of cycles. Therefore, the energy dissipation will be represented, as suggested by Hose and Seible (1999), by the area enclosed within the inelastic load-displacement curve and the unloading curve for each displacement cycle.

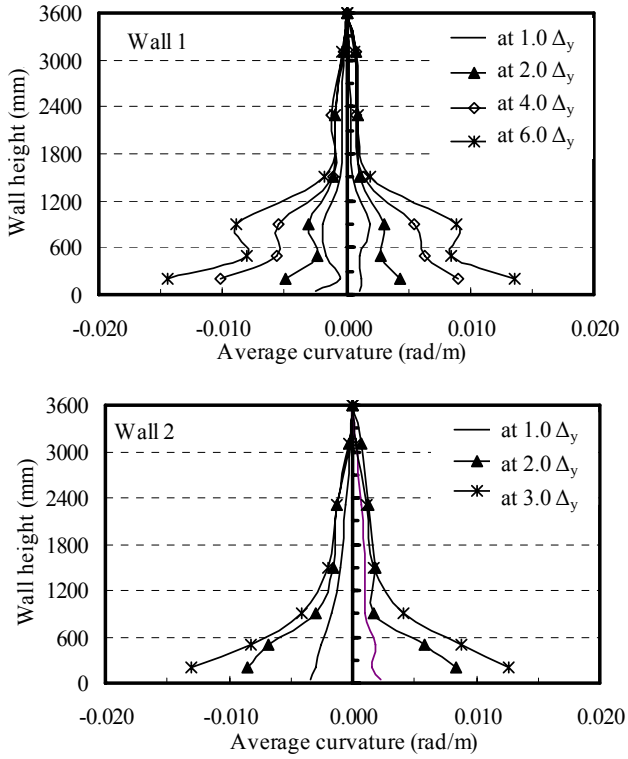

Figure 4 Curvature profiles along wall height

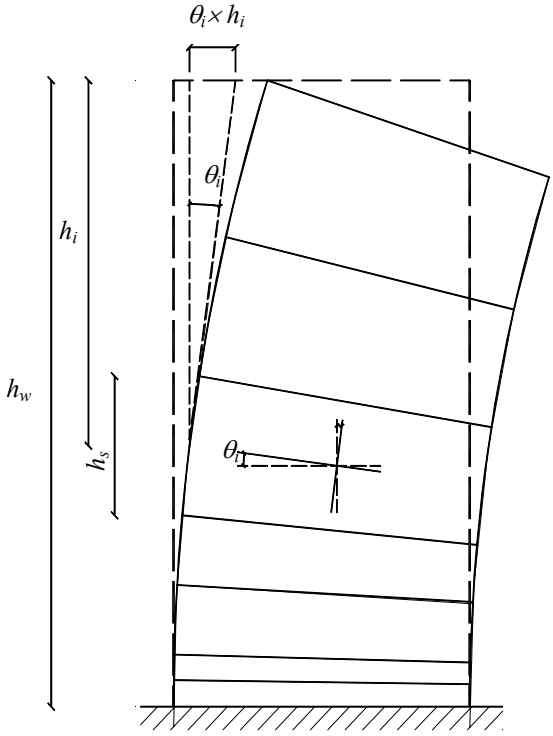

Figure 5 Flexure displacement calculation

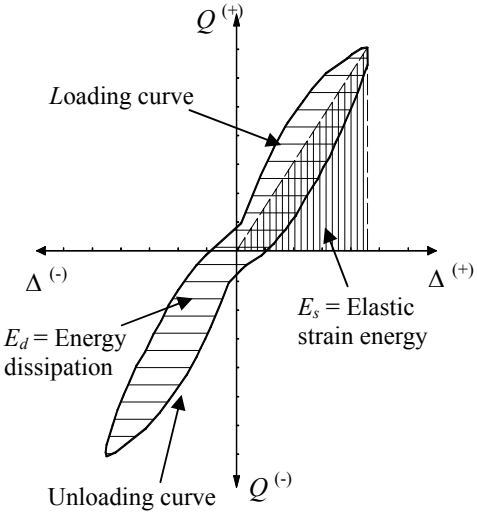

Figure 6 Energy dissipation calculation

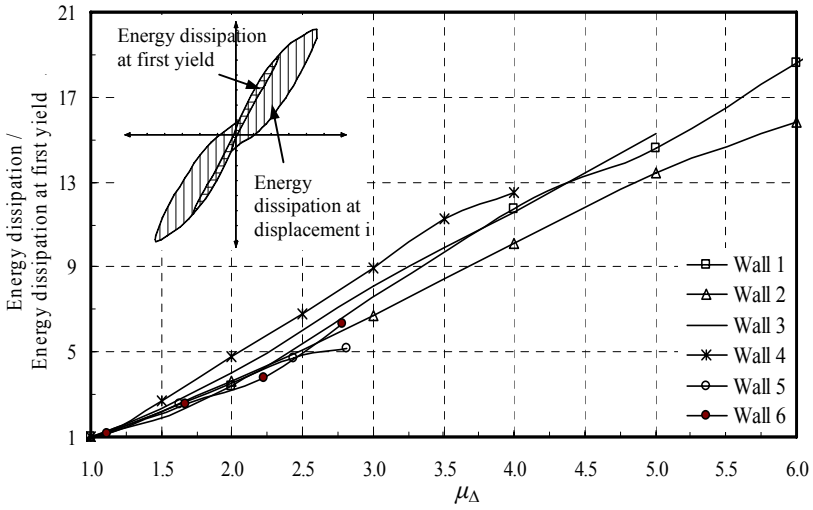

Figure 7 Normalized energy dissipation versus displacement ductility

The normalized energy dissipation values for the walls at different displacement levels, defined as the ratio between the energy dissipation at a certain displacement level beyond yield and the calculated energy dissipation at the onset of yielding are plotted versus the corresponding displacement ductilities in Fig. 7. Energy dissipation was normalized for individual walls to monitor the trend of increase of energy dissipation after yielding and to eliminate the effects of different wall capacities and displacement capabilities. The figure shows that, as expected, for low displacement levels, the energy dissipation was low which characterized the condition before significant yielding of the vertical reinforcement and significant inelastic deformation in the masonry had taken place. For higher displacement levels, the energy dissipation increased significantly with an almost linear increase in the amount of

energy dissipated associated with the increasing displacement ductility of the wall. The energy dissipation at a displacement of 2.5 times the yield displacement for the test walls is at least 5 times the dissipated energy at first yield.

4. CONCLUSION

All walls exhibited reasonably symmetric load-displacement relationships in both directions of loading until toe compression crushing occurred. The behavior of the walls was characterized by concentration of rotation over the lower part of the wall and relatively rigid body deformation for the upper part of the wall.
The flexural strength of reinforced masonry shear walls failing in flexure is very sensitive to the amount of vertical reinforcement and less sensitive to the increased axial compressive stress.
Flexure strength of reinforced masonry shear walls predicted using the Canadian and the American codes is in good agreement with the experimental results, except for walls subjected to high axial compressive stress.
Shear displacement, for flexurally dominated reinforced masonry shear walls with aspect ratio of 2.0, can on average be about 32% and 20% of the total lateral displacement at the onset of yielding of the outermost vertical bar and at maximum load, respectively.
The energy dissipated from hysteretic behavior of the walls subjected to large displacements increased significantly compared to early stages of loading and was proportional to the displacement ductility of the walls.

5. ACKNOWLEDGMENT

The financial support of the McMaster University Centre for Effective Design of Structures (*CEDS*) funded through the Ontario Research and Development Challenge Fund (*ORDCF*) is greatly appreciated. Provision of mason time by Ontario Masonry Contractors Association and Canada Masonry Design Centre is appreciated. The supply of concrete blocks and grout by Boehmer Block Ltd. is gratefully acknowledged.

6. REFERENCES

Abrams, D., (1986), Measured hysteresis in a masonry building system. Proceedings of the third U.S. Conference on Earthquake Engineering, Charleston, South Carolina, August.

Canadian Standards Association (CSA 2004). Design of masonry structures. CSA S304.1-04, Ontario, Canada.

Drysdale, R., and Hamid, A. (2005). Masonry structures- behaviour and design. First Canadian Edition, Canada Masonry Design Centre, Mississauga, ON, Canada.

Englekirk, R., and Hart, G. (1982). Earthquake design of concrete masonry buildings. Response spectra analysis and general earthquake modeling considerations, Vol. 1, Prentice Hall, Inc., Englewood Cliffs, N.J., USA.

Eurocode 8 (EC8) Design of structures for earthquake resistance Part 1: General rules, seismic actions and rule for buildings. prEN 1998-1, CEN, 2003, Brussels.

Hose, Y. and Seible, F. (1999). Performance evaluation database for concrete bridge components, and systems under simulated seismic loads. PEER report 1999/11, Pacific Earthquake Engineering Research Center College of Engineering, University of California, Berkley, U.S.A.

Masonry Standards Joint Committee (MSJC 2005). Building code requirements for Masonry Structures. ACI 530/ASCE 5 /TMS 402, American Concrete Institute, American Society of Civil Engineers, and The Masonry Society, Detroit, New York, and Boulder.

NBCC (2005). National Building Code of Canada, Institute for Research in Construction, National Research Council of Canada, Ottawa, ON, Canada.

Priestley, M. (1986). Seismic design of concrete masonry shear walls. *American Concrete Institute Structural Journal*, **(83) 1**, 58-68.

Priestley, M., and Park, R. (1987). Strength and ductility of concrete bridge columns under seismic loading. *American Concrete Institute Structural Journal,* **(84) 1**, 61-76.

Shedid, M. (2006). Ductility of reinforced concrete masonry shear walls. M.A.Sc. Thesis, Department of Civil Engineering, McMaster University, Ontario, Canada,.

Sinha, B., Gerstle, K., and Tulin, L. (1964). Stress-strain behavior for concrete under cyclic loading. *American Concrete Institute Structural Journal*, **(61) 2**, 195-211.